Journal of Korean Association of Crystal Growth
Vol. 5, No. 3 (1995) 240-249

Nonlinear optical properties of TiO_2 single crystal

Jae Heyg Shin and Keun Ho Orr
Department of Inorganic Materials Engineering, Hanyang University, Seoul 133-791, Korea

TiO_2 단결정의 비선형광학 특성

신재혁, 오근호
한양대학교 무기재료공학과, 서울, 133-791

Abstract Rutile type of TiO_2 single crystal was grown by floating zone method in order to obtain the highly transparent and contamination-free single crystal. The linear refractive index of perpendicular and parallel to c-axis was measured as a function of wavelength from 500 to 1000 nm. The optical energy band gap was estimated as 2.99 eV from the absorption spectrum. The theoretical $\chi^{(3)}$ value of TiO_2 was discussed in comparison with that of SiO_2 quartz single crystal on the basis of semiempirical model. On the other hand, the second-hyperpolarizability, $\gamma(Ti^{4+})$ was calculated in order to describe the effect of Ti^{4+} ion on the third order nonlinear optical properties.

요 약 무색투명하고 순수한 단결정을 얻기 위하여 TiO_2(rutile) 단결정을 floating zone법으로 성장하였다. 성장된 결정을 c축에 수직 및 수평하게 절단하여 500~1000 nm 범위의 파장에서 선형 굴절율을 측정하였으며 흡수스펙트롬으로부터 optical energy band gap이 2.99 eV임을 알 수 있었다. TiO_2(rutile) 단결정의 $\chi^{(3)}$ 값을 반경험적인 모델을 기반으로 하여 SiO_2 quartz 단결정의 $\chi^{(3)}$ 값과 비교하여 분석하였다. 또한 제 3 비선형광학 특성에 있어서의 Ti^{4+}의 영향을 해석하기 위해 second hyperpolarizability, $\gamma(Ti^{4+})$를 계산하였다.

1. Introduction

Nonlinear optical properties of materials have steadily increased in importance since the invention of the laser. The third order nonlinearity has also become of increasing

interest because of its effects on optical propagation of intense beams and its rapidly proliferating importance and applications in modern optical technology.

As recently reported, TiO_2 is also considered to be a promising nonlinear optical material because of the high refractive index more than about 2.5 and high transparency in the visible range [1]. In fact, $\chi^{(3)}$ values of 1.5×10^{-12} and 3.1×10^{-12} esu for a TiO_2 single crystal, which were measured by degenerate three-wave mixing [2] and degenerate four-wave mixing methods [3,4], respectively, have been reported.

In the present study, we have tried to grow a rutile type of TiO_2 single crystal by floating zone method and made measurements of various optical properties, such as refractive index (n_o and n_e) transmittance and energy gap. On the other hand, microscopic second hyperpolarizability and nonlinear refractive index were calculated from the refractive index and number density. Finally, the theoretical $\chi^{(3)}$ value of TiO_2 was discussed in comparison with that of SiO_2 quartz single crystal on the basis of semiempirical model and the results are discussed based on the semiempirical model in which an influence of second hyperpolarizability for cation on the nonlinear optical properties was taken into account.

2. Experimental

2.1. Crystal growing

High purity TiO_2 powder (99.99 %, Rare Earth Metal Co.) was used as starting material. The powder was sealed in a rubber tube and cold isostatic pressed into a rod, typically 12 mm in diameter and 70 mm in length with hydrostatic pressure of 2000 Kgf/cm^2. The pressed feed rod was sintered in box furnace at 1200℃, for 2 hr. After sintering, the dimensions of fed rod were 10 mm diameter and 60 mm length. A FZ-grown crystal was used for a seed crystal, which was cut parallel to the c-axis after the determination of orientation by Laue back scattering technique. The sintered rod and seed crystal were fixed to upper and lower shaftt respectirely. The growth machine (Asgal FZSS-10W) was infrared convergence type with double ellipsoidal reflectors. Two halogen lamps of 3.5 kW were used as heating source. The growth atmosphere was controlled by flowing air in 2 ℓ/min [5]. The growth condition were fixed to as follows : growth rate 5 mm/hr and counter-rotation rate of feed and seed 30 rpm respectively. For characterization, the single crystals of rutile type were cut to a thickness of 1.3 mm perpendicular to and parallel to the growth direction and then optically polished to eliminate light scattering at the surface. The final thickness of the TiO_2 single crystal was 1 mm.

2.2. Characterization

The linear refractive indices of these single crystals were measured as a function of wavelength in the range from 500 to 1000

nm using a spectroscopic ellipsometer.

The UV-visible spectra were measured over a wide wavelength range from 200 to 2000 nm using a Hitachi model U-3500 spectrophotometer.

3. Results

3.1. Linear refractive index

TiO_2 single crystal prepared in this study was optically transparent and colorless. The refractive index of perpendicular to c-axis (a) and of parallel to c-axis (b) are shown as a function of wavelength in Fig. 1 and Table 1. Hereafter, the refractive index of perpendicular to c-axis and of parallel to c-axis are presented simply as n_o and n_e, respectively for brevity.

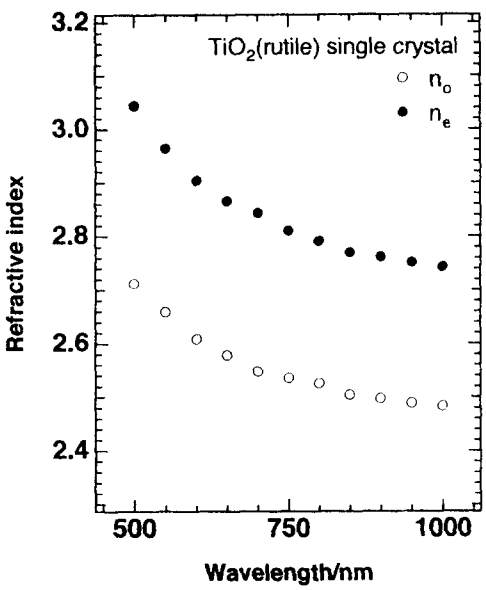

Fig. 1. Variation of refractive index of perpendicular to C-axis(n_o) and of parallel to c-axis(n_e) with wavelength in rutile type of TiO_2 single crystal.

Table 1
Refractive index, n_o and n_e of rutile type of TiO_2 single crystal

Wavelength/nm	n_o	n_e
500	2.712	3.044
550	2.659	2.964
600	2.608	2.904
650	2.578	2.866
700	2.547	2.844
750	2.535	2.810
800	2.525	2.791
850	2.504	2.770
900	2.497	2.762
950	2.489	2.752
1000	2.483	2.742

For comparison, the refractive index, n_o and n_e of quartz crystal are also plotted as shown in Fig. 2.

The refractive index decreased monotonously with increasing wavelength in the range from 500 to 1000 nm and were found to follow the Wemple relation [6] given below,

$$\frac{1}{n^2-1}=\frac{E_o}{E_d}-\frac{E^2}{E_o\cdot E_d} \quad (1)$$

where n is the refractive index, E the photon energy ($=h\nu$), E_o the average excitation energy for electrons equal to the Sellmeier gap [7] and E_d the electronic oscillator strength in eV unit.

Figure 3 (a) and (b) presents linear plots

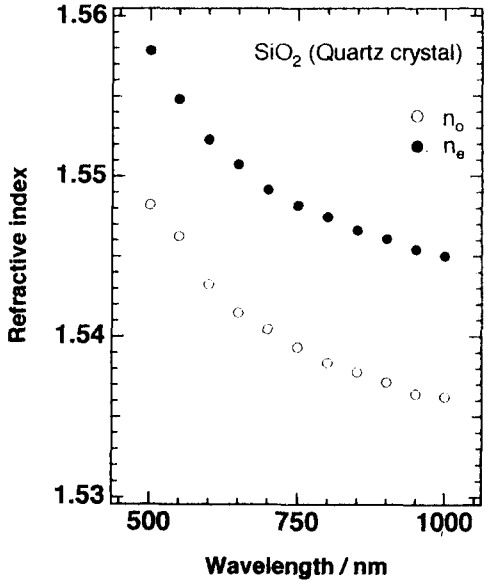

Fig. 2. Variation of refractive index of perpendicular to C-axis(n_o) and of parallel to c-axis(n_e) with wavelength in rutile type of SiO_2 (quartz) crystal.

of $(n^2-1)^{-1}$ versus E^2. The parameters, E_o and E_d, are determined by a linear fitting, this relation allows us to evaluate refractive indices at desired wavelengths. The calculated values of n_ω at wavelength of the 1900 nm are listed in Table 2 together with the E_0 and E_d values obtained using Eq. (1)

The Abbe number defined by $v_\delta = (n_d - 1)/(n_F - n_C)$ can also be calculated using Eq. (1), where n_F, n_d and n_c represent the refractive index at wavelengths of 486.1, 587.6 and 656.3 nm, respectively. The result is listed in Table 2, also.

3.2. *Transmittance*

Figure 4 shows the transmittance spectra of TiO_2 single crystal. Optical band gap (E_g)

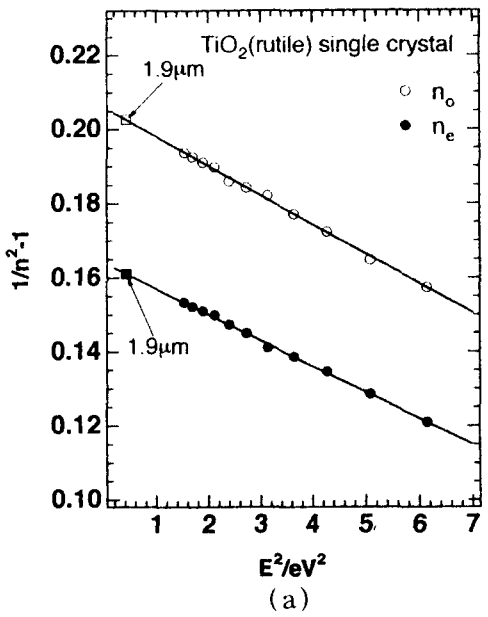

(a)

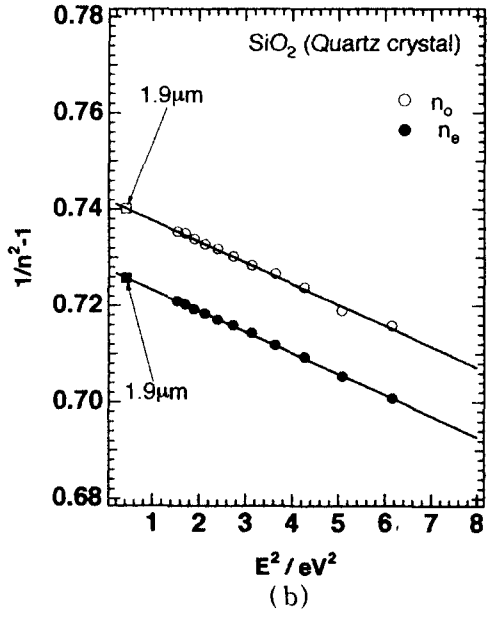

(b)

Fig. 3 (a) Dependence of refractive index n_o and n_e on photon energy in TiO_2 (rutile) single crystal and (b) Dependence of refractive index n_o and n_e on photon energy in SiO_2 (quartz) crystal.

Table 2
Optical properties of TiO_2 (rutile) single crystal and other nonlinear optical materials

Material	TiO_2	TiO_2	TiO_2	SiO_2	SiO_2
Type	rutile/ crystal/n_o	rutile/ crystal/n_e	rutile/ thin film	quartz/ crystal/n_o	quartz/ crystal/n_e
n_ω	2.44	2.68	2.27*	1.53	1.54
E_o/eV	5.10	4.84	5.10	13.10	13.01
E_d/eV	24.8	29.5	20.7	17.6	17.9
E_g/eV	2.99		3.01	8.40	
Bond length d/Å	1.96	1.96	1.96	1.61	1.61
Density D/gcm^{-3}	4.26	4.26	4.23	2.65	2.65
$\gamma/10^{-35}$ esu cm^3	2.919	3.547	2.678	0.170	0.175
$\chi^{(3)}_{miller}/10^{-12}$ esu	2.4	5.9	1.2	0.0131	0.0142
$\chi^{(3)}_{Lines}/10^{-12}$ esu	3.8	8.4	2.3	0.0165	0.0175
Abble number V_d	10.11	9.09	8.96	68.17	66.96
$n_{(2)}/10^{-13}$ esu	186.6	341.4	135.5	1.17	1.24

* 1 (see Ref. 16).

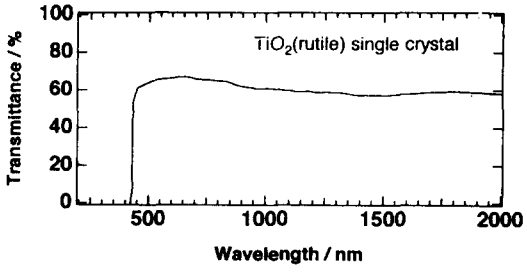

Fig. 4. Variation of transmittance with wavelength (nm) in TiO_2 (rutile) single crystal with 1 mm thickness.

of rutile type crystal was estimated from the extrapolation of a linear portion of the $(\alpha hv)^2$ vs hv plot to the (hv) axis as shown in Fig. 5. The values obtained are summarized in Table 2, also.

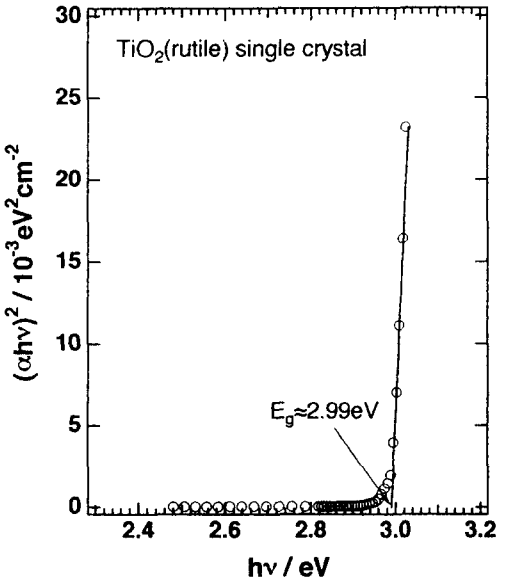

Fig. 5. Variation of $(\alpha hv)^2$ with hv in TiO_2 (rutile) single crystal with 1 mm thickness.

4. Discussion

4.1. Relationship between $\chi^{(3)}$ and refractive index

It is possible to estimate $\chi^{(3)}$ of a material from refractive index according to Miller's rule [8,9]

$$\chi^{(3)} = [\chi^{(1)}]^4 \times 10^{-10} \quad (2\text{-a})$$

and

$$\chi^{(1)} = \frac{n^2 - 1}{4\pi} \quad (2\text{-b})$$

The $\chi^{(3)}$ value calculated for rutile type of TiO_2 single crystal from Miller's rule was as high as 2.4×10^{-12} esu, about 180 times as large as that of SiO_2 quartz single crystal. Figure 6 shows a relationship between $\chi^{(3)}$ and refractive index, n_ω at 1900 nm rutile type of TiO_2 single crystal. For comparison, $\chi^{(3)}$ values of quartz and sapphire crystal, and anatase and rutile type of TiO_2 thin film are also plotted. It is seen that inorganic materials with high refractive index inherently exhibit high optical nonlinearity.

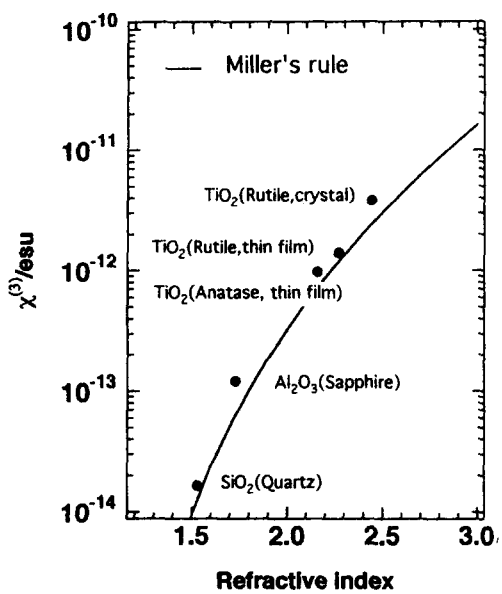

Fig. 6. Relationship between $\chi^{(3)}$ and refractive index (n_ω) for TiO_2 (rutile) single crystal and other nonolinear optical materials such as SiO_2 (quartz), Al_2O_3 (sapphire), rutile and anatase type of TiO_2 thin film.

4.2. Relationship between $\chi^{(3)}$ and optical band gap

An enhancement in $\chi^{(3)}(-3\omega\,;\,\omega,\,\omega,\,\omega)$ occurs when in a material a frequency of interacting light approaches either one of one, two or three photon resonance frequencies as follows [10].

$$\chi^{(3)}(-3\omega\,;\,\omega,\omega,\omega) \propto \frac{N}{\hbar} \sum_{gnm n'} \rho(g) \cdot F(\omega) \cdot \Omega_{gn}\,\Omega_{nm}\,\Omega_{mn'}\,\Omega_{n'g}\,(\text{esu}) \quad (3\text{-a})$$

and

$$F(\omega) = \frac{1}{(E_{ng} - 3\omega) \cdot (E_{mg} - 2\omega) \cdot (E_{n'g} - \omega)} + \frac{1}{(E_{ng} + \omega) \cdot (E_{mg} - 2\omega) \cdot (E_{n'g} - \omega)} + \frac{1}{(E_{ng} + \omega) \cdot (E_{mg} + 2\omega) \cdot (E_{n'g} - \omega)} + \frac{1}{(E_{ng} + \omega) \cdot (E_{mg} + 2\omega) \cdot (E_{n'g} + 3\omega)} \quad (3\text{-b})$$

where $\rho(g)$, E_{ij} and Ω_{ij} are the density matrix element of fundamental state, the ener-

gy difference between states i and j in $\hbar$ ($= h/2\pi$, h is the Planck's constant) unit and the transition matrix elements between states i and j, respectively. For materials having optical band gap, E_g, higher than three photon energy, 3ω, the three photon resonance makes the greatest contribution to the enhancement of $\chi^{(3)}$. Then, to a good approximation, the most significant term due to the three-photon resonance in above equation may be expressed as follow,

$$\chi^{(3)} = \frac{A}{(E_g-1.96)\cdot(E_g-1.31)\cdot(E_g-0.65)} \text{ (esu)} \quad (4)$$

where A is the phenomenological constant.

In Fig. 7, the $\chi^{(3)}$ is plotted as a function of optical band gap, E_g for rutile type of TiO_2 single crystal and other nonlinear optical materials. It is clearly seen that the smaller the optical band gap, the larger the value $\chi^{(3)}$. Furthermore, in this figure, the $\chi^{(3)}$ values of these materials show a clear tendency to increase asymptotically as the E_g approachs 1.96 eV corresponding to the photon energy of THG signal. This change obeys Eq. (4) when the parameter, A takes a value of 0.8×10^{-11}. The above result indicates that the large $\chi^{(3)}$ value of 2.4×10^{-12} esu for rutile type of TiO_2 single crystal, which is comparable to those for SiO_2 quartz single crystal (0.01×10^{-12} esu) and rutile type of TiO_2 thin film (1.2×10^{-12} esu), is explained by the two effects, the higher refractive index and the narrow optical band gap compared with SiO_2 quartz single crystal. In other words, the $\chi^{(3)}$ value for rutile type of TiO_2 single crystal is two order of magnitude higher than that of SiO_2 quartz.

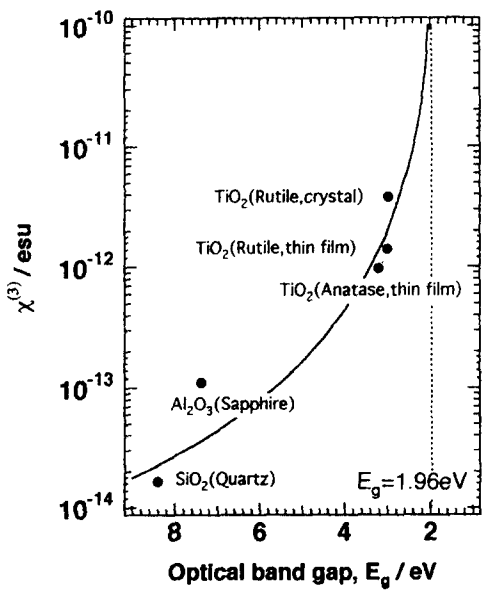

Fig. 7. Relationship between $\chi^{(3)}$ and optical band gap.

4.3. Theoretical $\chi^{(3)}$ value based on semiempirical model

Based on the bond-orbital theory [11], considered the contributions of cationic empty d-orbitals in addition to conduction band sp-orbitals to linear electronic polarization. It was found that the virtual electronic transitions to the empty d-orbitals and the sp-orbitals are essentially additive, that is, the dielectric constant $\varepsilon(\approx n^2)$ can be expressed as,

$$\varepsilon - 1 = 4\pi\chi^{(1)}_{sp} + 4\pi\chi^{(1)}_{d} \quad (5)$$

where $\chi^{(1)}_{sp}$ and $\chi^{(1)}_{d}$ are the sp- and d-elec-

tron polarizabilities, respectively. By using a theoretical expression derived for the long-wavelength sp electronic response of pretransition-metal compounds MX_n, the $\chi^{(1)}_{sp}$ is calculated as follows,

$$4\pi\chi^{(1)}_{sp} = \frac{|Z_x|^{1.5} \cdot n \cdot d^{4.4}}{4V_m}(1 + 0.65\frac{\Delta}{d})^2 \quad (6)$$

where

$$\Delta/d = \sqrt{(d/2r_M)} - 1, \quad (7)$$

Z_x is anionic valance, V_m the molar volume, d the M-X bond length (in Å) and r_M the cationic radius. Then, the d-orbital contribution, $4\pi\chi^{(1)}_d$, can be estimated from Eq. (5). The results were obtained by Lines [12] for the these three series of pretransition and transition metal oxides. $4\pi\chi^{(1)}_d$, is negligible for the pretransition metal oxides, but increases in magnitude as going to the right in the periodic table, explicitly corresponding to a decrease in M-O bond length. Such behavior is completely opposite to what is observed for $\chi^{(1)}_{sp}$ without d-orbital contributions. In case of sp-orbitals, a reduction of the anion-cation bond length causes an increment of the band gap energy between the bonding and antibonding orbitals leading to a lowering of $\chi^{(1)}_{sp}$, which is also expected from Eq. (6). Contrarily, the increase of $\chi^{(1)}_d$ with decreasing M-O bond length is possibly due to increasing $<d|p>$ overlapping.

TiO_2 (rutile) has the greatest $4\pi\chi^{(1)}_d$ as well as ε values of all the other oxides. These explain that the TiO_2 is exhibit the highest refractive index of all, while the SiO_2 quartz crystal show the lowest index.

In short, it is found based on the bond-orbital model that the virtual electronic transitions to the empty d-orbitals make a significant contribution to the refractive indices of optically transparent TiO_2 (rutile) single crystal.

Next, we will make an attempt to interpret systematically the $\chi^{(3)}$ values of the TiO_2 (rutile) single crystal in terms of physical quantities experimentally available. Based on the bond-orbital theory and the empirical observation of a great number of ionic and less ionic (covalent) crystals, Lines [11,12] derived a very simple semiquantitative expression for $n_2(av.)$ in the form of

$$n_2(av.) = \frac{L \cdot f_L^3 \cdot (n_\omega^2 - 1) \cdot d^2 \cdot E_s^6}{n_\omega (E_s^2 - E^2)^4} \text{ (esu)} \quad (8)$$

where f_L is the Lorentz field factor ($(n_\omega^2 + 2)/3$), n_ω the refractive index at wavelength ω, E_s the Sellmeier gap which is in practice equal to the average oscillator energy, E_o, in Eq. 1, E the photon energy ($h\nu$) and d the M-O bond length. The nonlinear refractive index $n_2(av.)$ is related to the third order nonlinear susceptibility $\chi^{(3)}$ via the next equation

$$\chi^{(3)} = \frac{n_\omega}{3\pi} \cdot n_2\,(av.)\ \text{(esu)} \quad (9\text{-a})$$

and

$$\chi^{(3)} = \frac{25 \times 10^{-13} \cdot f_L^3 \cdot (n_\omega^2 - 1) \cdot d^2 \cdot E_s^6}{3\pi(E_s^2 - E^2)^4} \text{ (esu)} \quad (9\text{-b})$$

From the Eq. (9), we can well predict the theoretical $\chi^{(3)}$ value in excellent agreement with the experimental result as reported previous paper [13,14]. The results were tabulated in Table 2.

Therfore, the much higher $\chi^{(3)}$ value for rutile type of TiO_2 single crystal compared with SiO_2 quartz can be ascribed to the higher refractive index and the narrower optical band gap or Sellmeier gap, which all result from the significant contribution of Ti 3d orbital due to the large p-d overlapping in the short Ti-O bond length of 1.96 Å.

4.4. Effect of Ti ion on third-order nonlinearity

In order to make the effect of valence of Ti ions on the third order nonlinear optical properties clear, microscopic second-hyperpolarizability, γ, is taken into account, because macroscopic $\chi^{(3)}$ depends on both γ_i, and the number density, N_i of the i th constituents as follows [15, 16],

$$\chi^{(3)} = \frac{f_L^4}{24} \cdot \sum_i N_i \cdot \gamma_i \text{ (esu)} \qquad (10)$$

For a metal oxide, M_xO_y, γ per $M_{x/y}O$ formula unit, $\gamma(M_{x/y}O)$, can be derived as follows,

$$\gamma_i(M_{x/y}O) = \frac{1944 \cdot \chi^{(3)} \cdot M_w}{N_A \cdot (n_\omega^2 + 2)^4 \cdot y \cdot D} \text{ (esu cm}^3\text{)} \qquad (11)$$

where M_w, D and N_A are the molecular weight and density of M_xO_y and Avogadro's number, respectively. The $\gamma(Ti^{4+} = 2.92 \times 10^{-35})$ of rutile type of TiO_2 single crystal is higher than those or $\gamma(Si^{4+} = 0.17 \times 10^{-35})$. Therefore, it can be said that the $\chi^{(3)}$ value of rutile type of TiO_2 single crystal may be governed by the second-hyperpolarizability, $\gamma(Ti^{4+})$.

5. Conclusion

Linear and nonlinear optical properties of rutile type of TiO_2 single crystal were discussed on the basis of semiempirical model. The results obtained are summarized as follows.

(1) The largest refractive index of 2.44 (n_o) was obtained for rutile type of TiO_2 single crystal.

(2) The optical energy band gap was estimated as 2.99 eV from the absorption spectrum.

(3) The $\chi^{(3)}$ value calculated for rutile type of TiO_2 single crystal from Miller's rule was as high as 2.4×10^{-12} esu, about 200 times as large as that of SiO_2 (0.01×10^{-12} esu) quartz single crystal.

(4) The $\chi^{(3)}$ value of rutile type of TiO_2 single crystal may be governed by the second-hyperpolarizability, $\gamma(Ti^{4+})$.

(5) The much higher $\chi^{(3)}$ value for rutile type of TiO_2 single crystal compared with SiO_2 quartz can be ascribed to the higher refractive index and the narrower optical band gap or Sellmeier gap, which all result from the significant contribution of Ti 3d orbital due to the large p-d overlapping in the short

Ti-O bond length of 1.96 Å.

References

[1] E.M. Vegel, J. Am. Ceram. Soc. 72 (1989) 719.

[2] R. Adir, L.L. Chase and S.A. Payne, Phys. Rev. B39 (1989) 3337.

[3] E.M. Vogel, S.G. Kosinski, D.M. Krol, J.L. Jakel, S.R. Friberg, M.K. Olier and J.D. Powers, J. Non-Cryst. Solids 107 (1989) 244.

[4] E.M. Vogel, M.J. Weber and D.M. Kr ol, Phys. Chem. Glass 32 (1991) 231.

[5] J.H. Shin, S.M. Kahng and K.K. Orr, J. Kor. Ceram. Soc. 27 (1990) 1050.

[6] S.H. Wemple, J. Chem. Phys. 67 (19-77) 2151.

[7] S.H. Wemple and M. Didomenico, Jr., Phys. Rev. B3 (1971) 338.

[8] R.C. Miller, Appl. Phys. Lett. 5 (1964) 17.

[9] C.C. Wang, Phys. Rev. B2 (1970) 2045.

[10] F. Kaizar and J. Meseier, Nonlinear Optical Properties of Organic Molecules and Crystals, 2, Ed by D.S. Chemia and J. Zyss (Academic Press, New York, 1970) p. 51.

[11] M.E. Lines, Phys. Rev. B43 (1991) 11978.

[12] M.E. Lines, Ohys. Rev. B41 (1990) 3383

[13] S.H. Kim, T. Yoko and S. Sakka, J. Am. Ceram. Soc. 76 (1993) 2486.

[14] S.H. Kim and T. Yoko, J. Am. Ceram. Soc. (1995) to be published.

[15] N.L. Boling, A.J. Glass and A. Owyoung, IEEE J. Quant. Electron., QE-14 (1978) 601.

[16] P.J. Martin, J. Mater. Sci. 21 (1986) 1.